

2017

# Mechanistic understanding of *N*-glycosylation in Ebola virus glycoprotein maturation and function

Bin Wang  
*CAAS-Michigan State University*

Yujie Wang  
*CAAS-Michigan State University*


Dylan A. Frabutt  
*Michigan State University*

Xihe Zhang  
*Michigan State University*

Xiaoyu Yao  
*CAAS-Michigan State University*

*See next page for additional authors*

Follow this and additional works at: <http://digitalcommons.unl.edu/vetscipapers>

 Part of the [Biochemistry, Biophysics, and Structural Biology Commons](#), [Cell and Developmental Biology Commons](#), [Immunology and Infectious Disease Commons](#), [Medical Sciences Commons](#), [Veterinary Microbiology and Immunobiology Commons](#), and the [Veterinary Pathology and Pathobiology Commons](#)

---

Wang, Bin; Wang, Yujie; Frabutt, Dylan A.; Zhang, Xihe; Yao, Xiaoyu; Hu, Dan; Zhang, Zhuo; Liu, Chaonan; Zheng, Shimin; Xiang, Shi-Hua; and Zheng, Yong-Hui, "Mechanistic understanding of *N*-glycosylation in Ebola virus glycoprotein maturation and function" (2017). *Papers in Veterinary and Biomedical Science*. 300.  
<http://digitalcommons.unl.edu/vetscipapers/300>

This Article is brought to you for free and open access by the Veterinary and Biomedical Sciences, Department of at DigitalCommons@University of Nebraska - Lincoln. It has been accepted for inclusion in Papers in Veterinary and Biomedical Science by an authorized administrator of DigitalCommons@University of Nebraska - Lincoln.


---

**Authors**

Bin Wang, Yujie Wang, Dylan A. Frabutt, Xihe Zhang, Xiaoyu Yao, Dan Hu, Zhuo Zhang, Chaonan Liu, Shimin Zheng, Shi-Hua Xiang, and Yong-Hui Zheng

# Mechanistic understanding of *N*-glycosylation in Ebola virus glycoprotein maturation and function

Received for publication, November 15, 2016, and in revised form, February 12, 2017. Published, JBC Papers in Press, February 14, 2017, DOI 10.1074/jbc.M116.768168

Bin Wang<sup>†1,2</sup>, Yujie Wang<sup>†1</sup>, Dylan A. Frabutt<sup>5</sup>, Xihe Zhang<sup>5</sup>, Xiaoyu Yao<sup>‡</sup>, Dan Hu<sup>‡</sup>, Zhuo Zhang<sup>‡</sup>, Chaonan Liu<sup>¶</sup>, Shimin Zheng<sup>¶</sup>, Shi-Hua Xiang<sup>||</sup>, and  Yong-Hui Zheng<sup>‡5,3</sup>

From the <sup>†</sup>Harbin Veterinary Research Institute, CAAS-Michigan State University Joint Laboratory of Innate Immunity, State Key Laboratory of Veterinary Biotechnology, Chinese Academy of Agricultural Sciences, Harbin 150059, China, the <sup>¶</sup>College of Veterinary Medicine, Northeast Agricultural University, Harbin 150030, China, the <sup>||</sup>Nebraska Center for Virology and School of Veterinary Medicine and Biomedical Sciences, University of Nebraska, Lincoln, Nebraska 68583, and the <sup>5</sup>Department of Microbiology and Molecular Genetics, Michigan State University, East Lansing, Michigan 48824

Edited by Charles E. Samuel

The Ebola virus (EBOV) trimeric envelope glycoprotein (GP) precursors are cleaved into the receptor-binding GP<sub>1</sub> and the fusion-mediating GP<sub>2</sub> subunits and incorporated into virions to initiate infection. GP<sub>1</sub> and GP<sub>2</sub> form heterodimers that have 15 or two *N*-glycosylation sites (NGSs), respectively. Here we investigated the mechanism of how *N*-glycosylation contributes to GP expression, maturation, and function. As reported before, we found that, although GP<sub>1</sub> NGSs are not critical, the two GP<sub>2</sub> NGSs, Asn<sup>563</sup> and Asn<sup>618</sup>, are essential for GP function. Further analysis uncovered that Asn<sup>563</sup> and Asn<sup>618</sup> regulate GP processing, demannosylation, oligomerization, and conformation. Consequently, these two NGSs are required for GP incorporation into EBOV-like particles and HIV type 1 (HIV-1) pseudovirions and determine viral transduction efficiency. Using CRISPR/Cas9 technology, we knocked out the two classical endoplasmic reticulum chaperones calnexin (CNX) and/or calreticulin (CRT) and found that both CNX and CRT increase GP expression. Nevertheless, NGSs are not required for the GP interaction with CNX or CRT. Together, we conclude that, although Asn<sup>563</sup> and Asn<sup>618</sup> are not required for EBOV GP expression, they synergistically regulate its maturation, which determines its functionality.

The 2014 outbreak of Ebola hemorrhagic fever in West Africa has resulted in the deaths of over 11,000 people and represents the worst epidemic of this disease in history (1). Ebola hemorrhagic fever is caused by Ebola viruses (EBOVs),<sup>4</sup>

members of Filoviridae, which can have a 90% rate of mortality in humans and nonhuman primates (2). Filoviridae is composed of two genera: EBOVs and Marburg viruses, which are enveloped and have single, non-segmented, negative-sense RNA genomes with a size of ~19 kb (3). So far, five EBOV species have been identified, including Zaire, Sudan, Bundibugyo, Tai Forest, and Reston, which share ~60% amino acid identity. All of these isolates can cause diseases in humans, except for the Reston strain, which is pathogenic in nonhuman primates; the Zaire, Sudan, and Bundibugyo strains have been very pathogenic in humans (2).

The EBOV genome encodes seven structural proteins and one non-structural protein (3). As the only structural component on the viral surface, the glycoprotein (GP) is responsible for viral entry and initiation of infection (4, 5). EBOV GPs are class I viral fusion proteins, a classification category that also includes influenza viruses, paramyxoviruses, and retroviruses (6). EBOV GP is unique because it also functions as an important virulence factor that induces cytotoxic effects both *in vivo* and *in vitro* (7). Thus, EBOV has evolved an RNA-editing mechanism to regulate its GP expression through two open reading frames (8, 9). Most transcripts (80%) are not RNA-edited and thus produce a truncated, secreted GP because of a premature stop codon that plays a role in immune evasion (10). The remaining transcripts are edited, which produces the full-length precursor GP (GP<sub>pre</sub>) in the endoplasmic reticulum (ER). GP<sub>pre</sub> is further processed into a fully glycosylated uncleaved GP<sub>0</sub> that assembles into trimers in the ER. Each GP<sub>0</sub> subunit is then cleaved by the convertase furin in the *trans*-Golgi to produce the surface subunit GP<sub>1</sub> (~130 kDa) and transmembrane subunit GP<sub>2</sub> (~24 kDa), which are linked by a disulfide bond (11). Although the incorporation of GP trimers into viral particles is necessary for infection, many of these trimers are released into culture medium because of cleavage of the GP<sub>2</sub> transmembrane anchor by tumor necrosis factor  $\alpha$ -converting enzyme (12).

The authors declare that they have no conflicts of interest with the contents of this article. The content is solely the responsibility of the authors and does not necessarily represent the official views of the National Institutes of Health.

This article contains supplemental Table 1.

<sup>1</sup> Both authors contributed equally to this work.

<sup>2</sup> Supported by National Natural Science Foundation of China Grant 31502089 and Harbin Veterinary Research Institute Grant SKLVBP2015012. The authors declare that they have no conflicts of interest with the contents of this article.

<sup>3</sup> Supported by NIAID, National Institutes of Health Grants AI120189, AI106477, and AI122863. To whom correspondence should be addressed: Dept. of Microbiology and Molecular Genetics, Michigan State University, 2215 BPS, 567 Wilson Rd., East Lansing, MI 48824. Tel.: 517-884-5314; Fax: 517-353-8957; E-mail: zhengyh@msu.edu.

<sup>4</sup> The abbreviations used are: EBOV, Ebola virus; GP, glycoprotein; GP<sub>pre</sub>, precursor glycoprotein; ER, endoplasmic reticulum; MLD, mucin-like domain;

RBD, receptor-binding domain; NGS, *N*-glycosylation site; Man, mannose; CNX, calnexin; CRT, calreticulin; Env, envelope glycoprotein; HIV-1, HIV type 1; FL, full-length; Luc, luciferase; Endo H, endoglycosidase H; KIF, kifunessine; E-VLP, Ebola virus-like particle; SIV, simian immunodeficiency virus; RIPA, radioimmune precipitation assay.

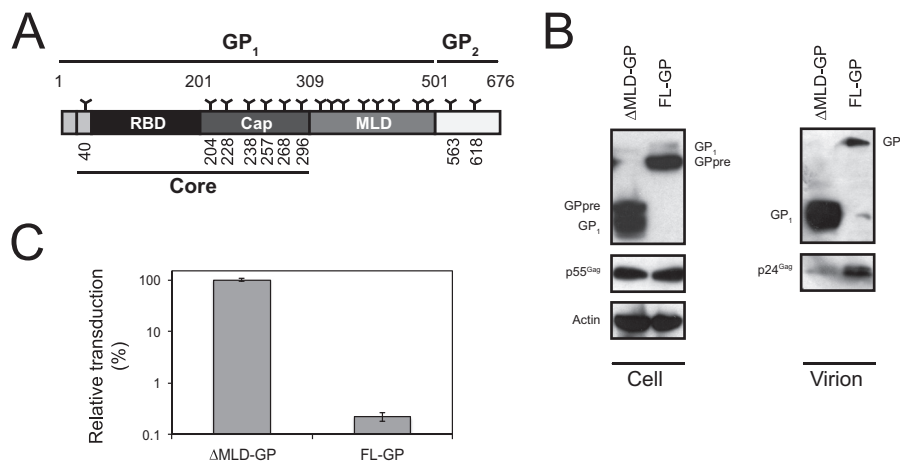


**Figure 1. A functional comparison of EBOV FL-GP and  $\Delta$ MLD-GP.** *A*, schematic of EBOV GP. GP<sub>1</sub>, GP<sub>2</sub>, core, MLD, RBD, and glycan cap (Cap) regions in FL GP are indicated. Numbers indicate amino acid residues. NGSs are marked as Y. *B*, FL-GP and  $\Delta$ MLD-GP expression in cells and their incorporation into HIV-1 virions were detected by Western blotting. GP<sub>pre</sub>, EBOV GP precursor; p24 and p55, HIV-1 Gag antigens. GP proteins were detected by an anti-FLAG antibody, and actin and HIV-1 Gag proteins were detected by their specific antibodies. *C*, comparison of GP-mediated HIV-1 transduction. Virions were produced from 293T cells after transfection with the pNL-Luc- $\Delta$ Env and  $\Delta$ MLD-GP or FL-GP expression vectors. Vero cells were infected with these viruses after normalization of the p24 Gag proteins, and viral transduction efficiency was quantitated by measuring the cellular luciferase activities. Results are presented as relative values. Error bars represent standard deviations calculated from three experiments.

GP<sub>1</sub> is divided into core domain and mucin-like domain (MLD), and the core domain is further divided into the receptor-binding domain (RBD) and glycan cap (Fig. 1A) (13). The MLD is responsible for the cytotoxic effect (7), and deletion of this domain increases GP processing and incorporation into retroviral particles, resulting in higher transduction efficiency (13). GP<sub>2</sub> contains an internal fusion loop, two heptad repeats (HR1 and HR2) connected by a functionally important linker, and a transmembrane domain. GP<sub>1</sub> is responsible for attachment to host cells, and GP<sub>2</sub> is responsible for mediating fusion of the virus envelope with the host endosomal membranes. In fact, EBOV infection requires minimal incorporation of GP on the surface of virions; increasing GP incorporation in virions can strongly reduce viral transduction efficiency (14).

Filovirus GPs are heavily glycosylated with both *N*-linked and *O*-linked glycans, and glycans contribute over one-third of their molecular weight (8). The Zaire EBOV GP<sub>1</sub> and GP<sub>2</sub> subunits have 15 or two *N*-linked glycosylation sites (NGSs) (Fig. 1A) (15). The MLD itself has eight NGSs and  $\sim$ 80 *O*-linked glycosylation sites (3). By pseudotyping the GP-defective vesicular stomatitis virus with EBOV GPs, it was reported that, although the 15 GP<sub>1</sub> NGSs protect EBOV from neutralizing antibodies, they are dispensable for GP expression and function (16). In contrast, the two GP<sub>2</sub> NGSs, Asn<sup>563</sup> and Asn<sup>618</sup>, are indispensable for EBOV GP-mediated vesicular stomatitis virus transduction (17). However, it remained unclear how Asn<sup>563</sup> and Asn<sup>618</sup> determine the GP function.

*N*-glycosylation starts in the ER on asparagine residues with a consensus NXS/T motif and is completed in the Golgi by adding a heterogeneous mixture of high-mannose (Man), hybrid, and complex oligosaccharides (18). This process involves a number of chaperones, glycoside hydrolases, and oxidoreductases to promote protein folding and maturation. Calnexin (CNX) and calreticulin (CRT) comprise a fundamental ER chaperone system, ensuring that glycoproteins achieve proper folding after glycosylation by interacting with their polypeptide

precursors in glycan-dependent or independent manners (19). Currently, it is still unclear whether EBOV GPs employ the CNX/CRT cycle for expression and how they interact with CNX/CRT.

Previously, envelope glycoprotein (Env)-defective ( $\Delta$ Env) murine leukemia viruses were pseudotyped with EBOV GPs to study their function (13). Here we used  $\Delta$ Env HIV type 1 (HIV-1) as a surrogate infection system to study EBOV GP *N*-glycosylation. In combination with site-directed mutagenesis and biochemical approaches, we have not only confirmed the important role of Asn<sup>563</sup> and Asn<sup>618</sup> but also collected mechanistic insight into why they are so critical for GP function.

## Results

### The role of Asn<sup>563</sup>/Asn<sup>618</sup> in GP processing and virion incorporation

To reduce cytotoxicity, we used MLD-deleted ( $\Delta$ MLD) GP in most of our experiments to study GP activity. We first compared  $\Delta$ MLD-GP expression and activity with the full-length (FL) GP. All GP proteins were fused to an N-terminal FLAG tag, so their expressions were detectable with an anti-FLAG antibody. 293T cells were transfected with an FL-GP or  $\Delta$ MLD-GP expression vector plus a  $\Delta$ Env HIV-1 proviral vector expressing the firefly luciferase report gene (pNL-Luc $\Delta$ Env). After 48 h, pseudovirions were collected and quantified, and the viral transduction efficiency was measured by infecting Vero cells. In addition, transfected cells as well as pseudovirions were lysed, and the levels of viral protein expression were determined by Western blotting.

As reported, we found that, because of the heavy *O*- and *N*-glycosylation of the MLD in the Golgi, FL-GP<sub>1</sub> exhibited a higher molecular weight than FL-GP<sub>pre</sub>, whereas  $\Delta$ MLD-GP<sub>1</sub> exhibited a lower molecular weight than  $\Delta$ MLD-GP<sub>pre</sub> (Fig. 1B). In addition,  $\Delta$ MLD-GP exhibited higher levels of protein expression and were more effectively processed and pack-

## Functional characterization of EBOV GP N-glycosylation

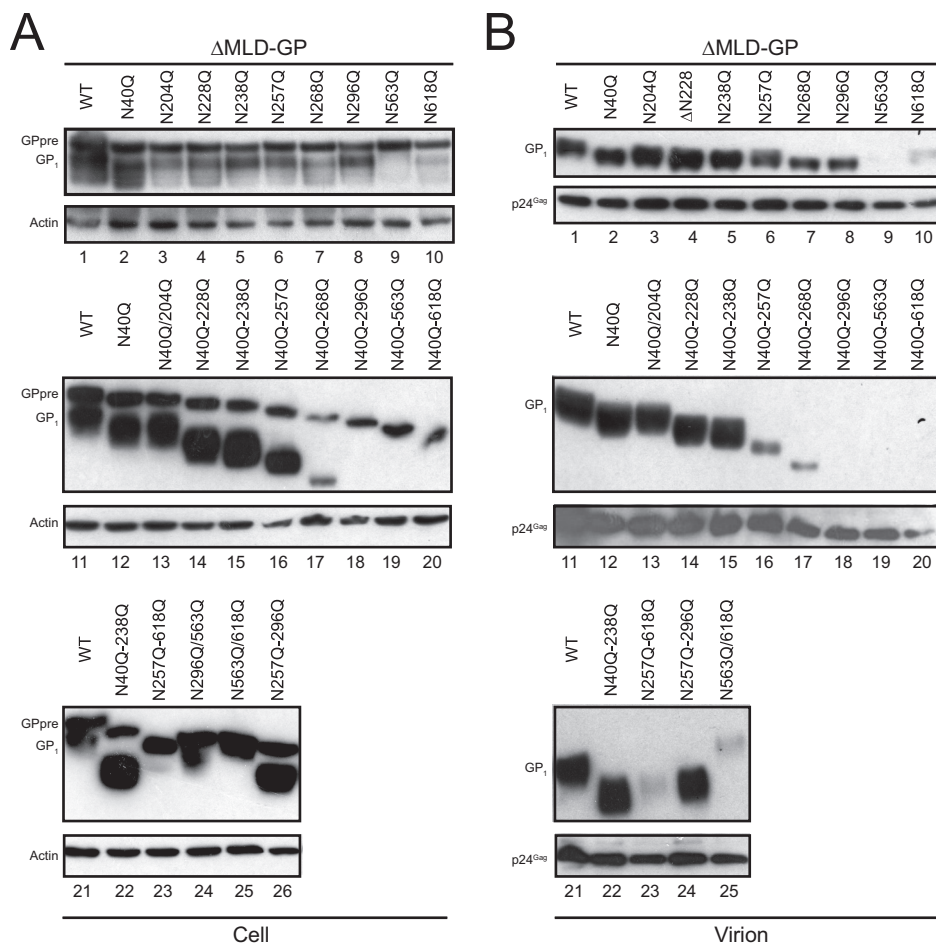


**Figure 2. Mutational analysis of EBOV GP NGSs.** A and B, 293T cells were transfected with the WT or the indicated  $\Delta$ MLD-GP mutant expression vectors. Virions were purified from cell culture supernatants by ultracentrifugation. Cells (A) and virions (B) were lysed and analyzed by Western blotting.

aged into HIV-1 particles than FL-GP (Fig. 1B). Moreover,  $\Delta$ MLD-GP dramatically increased HIV-1 transduction compared with FL-GP (Fig. 1C). These results demonstrate that  $\Delta$ MLD-GP provides a more effective and convenient system to study GP biochemistry and function.

Next, each of the nine NGSs on  $\Delta$ MLD-GP were deglycosylated by replacing Asn with Gln, creating nine mutants: N40Q, N204Q, N228Q, N238Q, N257Q, N268Q, N296Q, N563Q, and N618Q. When their expression in cells and HIV-1 pseudovirions was determined, it was found that none of these single mutations reduced GP expression and processing, except for N563Q and N618Q, which reduced processing (Fig. 2A, lanes 1–10). In addition, both the N618Q and N563Q mutations dramatically reduced GP incorporation (Fig. 2B, lanes 9 and 10).

To continue this investigation, a number of combinative and accumulative mutations were created. For example, N40Q/204Q, N296Q/563Q, and N563Q/618Q have the two indicated NGSs mutated; N40Q-228Q, N40Q-238Q, N40Q-257Q, N40Q-268Q, N40Q-296Q, N40Q-563Q, N40Q-618Q, N257Q-618Q, and N257Q-296Q have three to nine NGSs mutated. A more detailed description of these mutations is provided in supplemental Table 1. It was found that the five N-terminal NGSs (Asn<sup>40</sup> to Asn<sup>257</sup>) were not required for GP cleavage (Fig. 2A, lanes 11–16). However, when the accumulated mutations were extended to Asn<sup>268</sup> and beyond, GP<sub>1</sub> expres-

sion either decreased or became undetectable in both cells and virions (Fig. 2, A and B, lanes 17–20). When the five C-terminal NGSs (Asn<sup>257</sup>, Asn<sup>268</sup>, Asn<sup>296</sup>, Asn<sup>563</sup>, and Asn<sup>618</sup>) were mutated (N257Q–N618Q), GP<sub>1</sub> became undetectable in cells and virions (Fig. 2, A and B, lane 23); when Asn<sup>563</sup> and Asn<sup>618</sup> were mutated (N563Q/N618Q), GP<sub>1</sub> showed the same defect (Fig. 2, A and B, lane 25). Together, these results demonstrate that Asn<sup>563</sup>/Asn<sup>618</sup> are crucial for EBOV GP proteolytic cleavage and incorporation.

### Role of Asn<sup>563</sup>/Asn<sup>618</sup> in GP demannosylation

During N-glycosylation, the preassembled oligosaccharide (Glc<sub>3</sub>Man<sub>9</sub>GlcNAc<sub>2</sub>) needs to be further processed after being attached to NGSs. Among the nine Man residues, four are  $\alpha$ 1,2-linked and are sequentially removed by class I  $\alpha$ -mannosidases. The other five are either  $\alpha$ 1,3- or  $\alpha$ 1,6-linked, and two of these are removed by a class II  $\alpha$ -mannosidase. Endoglycosidase H (Endo H) cleaves each structure of these oligosaccharides as they are processed until the class II enzyme removes the two Man residues. Thus, Endo H-sensitive and -resistant glycoproteins contain high-Man or low-Man sugars, respectively.

We used Endo H treatment to determine how NGSs regulate GP demannosylation. As expected, GP<sub>pre</sub>s from both  $\Delta$ MLD-GP and FL-GP were sensitive to Endo H because it contains unprocessed Man residues; GP<sub>1</sub> was resistant to Endo H

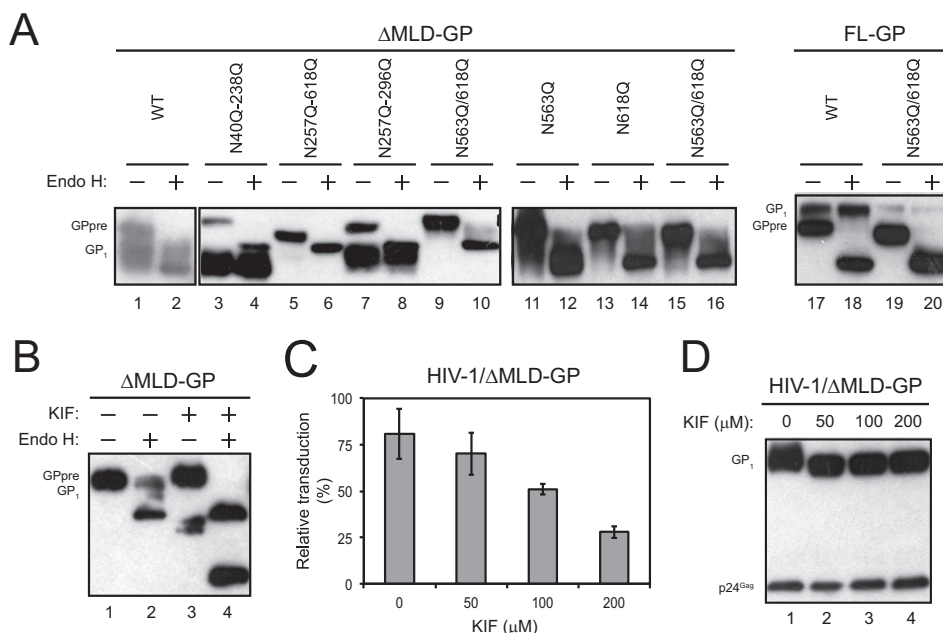


**Figure 3. Effect of demannosylation on EBOV function.** *A*, analysis of GP sensitivity to Endo H. 293T cells were transfected with the indicated GP expression vectors. Cell lysate was either treated with Endo H or left untreated and analyzed by Western blotting. *B*, KIF increases GP sensitivity to Endo H. 293T cells transfected with the  $\Delta$ MLD-GP expression vector were treated with 50  $\mu$ M KIF or remained untreated. Lysate from these cells was treated with Endo H or left untreated and analyzed by Western blotting. *C*, KIF inhibition of GP-mediated HIV-1 transduction. 293T cells producing HIV-1 luciferase reporter viruses pseudotyped with EBOV  $\Delta$ MLD-GP were treated with the indicated amounts of KIF. Viral transduction was measured by infecting Vero cells. Error bars represent standard deviation from three experiments. *D*, KIF does not affect GP expression in HIV-1 virions. HIV-1 pseudovirions produced in *C* were purified by ultracentrifugation, and viral protein expression in these virions was determined by Western blotting.

because its Man residues were already processed (Fig. 3*A*, lanes 1, 2, 17, and 18). Removal of the four N-terminal NGSs (Asn<sup>40</sup> to Asn<sup>238</sup>) or the three middle NGSs (Asn<sup>257</sup> to Asn<sup>296</sup>) increased the Endo H-resistant band (Fig. 3*A*, lanes 3, 4, 7, and 8), whereas removal of the five C-terminal NGSs (Asn<sup>257</sup> to Asn<sup>618</sup>) almost completely eliminated the Endo H-resistant band (Fig. 3*A*, lanes 5 and 6). Importantly, when Asn<sup>563</sup> and/or Asn<sup>618</sup> were removed (N563Q, N618Q, and N563Q/N618Q), the Endo H-resistant band was eliminated (Fig. 3*A*, lanes 9–16, 19, and 20). These results demonstrate that Asn<sup>563</sup> and Asn<sup>618</sup> are required for demannosylation.

To understand how demannosylation affects GP function, we treated cells with kifunesine (KIF), a potent inhibitor of class I mannosidases that is primarily used in cell culture to make high-Man glycoproteins (20). It was found that the treatment completely eliminated the Endo H-resistant EBOV GP, indicating that KIF effectively blocked demannosylation (Fig. 3*B*). In addition, KIF reduced HIV-EBOV GP transduction in a dose-dependent manner without reducing the levels of the GP incorporation (Fig. 3, *C* and *D*). These results demonstrate that demannosylation is required for EBOV GP function.

#### The role of Asn<sup>563</sup>/Asn<sup>618</sup> in GP oligomerization

To understand whether the N563Q and N618Q mutations have altered the GP conformation, we used flow cytometry to determine GP interaction with two conformation-dependent anti-EBOV GP mAbs, KZ52 (21) and 13C6 (22). We first used a conformation-independent anti-FLAG antibody to detect WT, N563Q, N618Q, and N563Q/N618Q  $\Delta$ MLD GP proteins and found a similar level of surface expression (Fig. 4, *A* and *B*). However, the N563Q mutation reduced KZ52 and 13C6

binding by 25% or 50%, and the N618Q mutation also did so at relatively modest levels (Fig. 4, *A* and *B*). These results are consistent with a previous report (17), suggesting that Asn<sup>563</sup>/Asn<sup>618</sup> are important for maintaining the natural conformation.

Next we tested whether Asn<sup>563</sup> and Asn<sup>618</sup> play a role in GP oligomerization. Asn<sup>563</sup> is located in the proximity of the trimer interface and may play a role in trimer stabilization (23, 24). The Asn<sup>618</sup> glycan is an unusual sugar that is present in the HR2 region, and the currently solved crystal structures of GP have not extended to this region. However, it is possible that this sugar might create some steric hindrance to trimer formation or stabilization.  $\Delta$ MLD-GP and its mutants N563Q, N618Q, or N563/618Q were expressed in 293T cells, and soluble GPs were purified from the culture medium. It was found that a single monomer GP band was detected at a similar level in the reducing gel, indicating that Asn<sup>563</sup> and Asn<sup>618</sup> are not required for GP shedding (Fig. 4*C*). However, a striking difference was found in the non-reducing gel. Trimers and monomers were detected from  $\Delta$ MLD-GP proteins at a ratio of 1.75:1, monomers were exclusively detected from N563Q, trimers were exclusively detected from N618Q, and trimers and monomers were also detected from N563Q/N618Q but at a ratio 0.44:1 (Fig. 4, *C* and *D*). These results demonstrate that Asn<sup>563</sup> increases, whereas Asn<sup>618</sup> inhibits, trimer formation, and the N563Q/N618Q double mutation results in an overall reduction in trimer formation.

#### Role of CNX/CRT in GP expression

CNX is a type I transmembrane protein with 592 amino acids, and CRT is its soluble paralog, sharing ~39% sequence

## Functional characterization of EBOV GP N-glycosylation

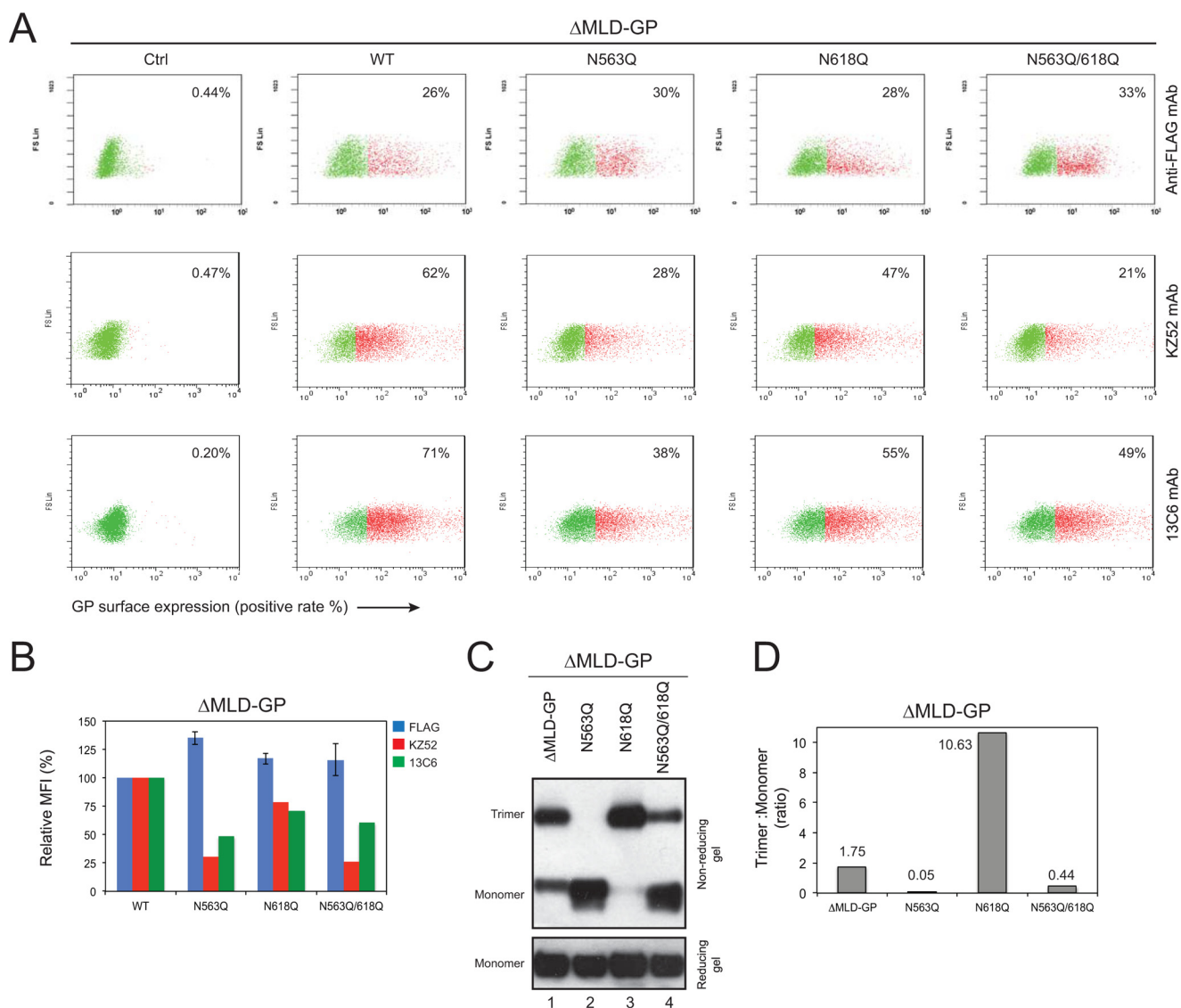


**Figure 4. Influence of Asn<sup>563</sup>/Asn<sup>618</sup> mutations on EBOV GP conformation.** *A* and *B*, detection of GP interaction with conformation-dependent neutralizing antibodies was performed using flow cytometry. 293T cells were transfected with the indicated expression vectors. Cells were stained with anti-FLAG, KZ52, or 13C6 antibodies and analyzed by FACSscan. The levels of positive populations are shown in *A*, and the mean fluorescence intensity (MFI) in these populations is shown in *B*. Error bars represent standard deviation calculated from three experiments. *Ctrl*, control. *C*, analysis of GP oligomerization. 293T cells were transfected with the indicated ΔMLD-GP expression vectors. Cellular proteins were resolved with non-reducing or reducing gels and analyzed by Western blotting. The trimer and monomer bands in the Western blot (C) was quantified with ImageJ. Their relative ratios were then calculated and are presented.

identity with 417 amino acids. Their role in EBOV GP biosynthesis has not been tested.

First, we determined whether EBOV GP expression depends on CNX/CRT. The *CNX* and/or *CRT* genes were knocked out from 293T cells using CRISPR/Cas9 technology (Fig. 5A), generating two single KO cell lines, Δ*CNX* and Δ*CRT*, and one double KO cell line, ΔΔ (Fig. 5B). When EBOV GP expression was determined in these KO cells, it was found that GP expression was reduced in both Δ*CNX* and Δ*CRT* cells, and the expression was further reduced in ΔΔ cells (Fig. 5C). In addition, when *CNX* and *CRT* expression was gradually restored in ΔΔ cells by co-transfection with their expression vectors, GP expression was increased in a dose-dependent manner (Fig. 5, D and E). These results demonstrate that both *CNX* and *CRT* increase EBOV GP expression.

Second, we determined whether EBOV GPs interact with *CNX* or *CRT*. ΔMLD-GPs were expressed in WT, Δ*CNX*, Δ*CRT*, and ΔΔ cells, and protein complexes were pulled down using anti-FLAG antibodies. It was found that the endogenous *CNX* could be pulled down from WT and Δ*CRT* but not Δ*CNX* and ΔΔ cells (Fig. 6A). These results demonstrate that GPs interact with *CNX* in a *CRT*-independent manner. To detect the interaction with *CRT*, these cells were co-transfected with a *CRT* expression vector, and the experiment was repeated. It was found that, although similar levels of *CRT* were detected in these cells, *CRT* could only be pulled down from cells expressing GPs (Fig. 6B). In addition, more *CRT* proteins were pulled down from WT and Δ*CNX* than Δ*CRT* and ΔΔ cells. These results demonstrate that GPs also interact with *CRT* in a *CNX*-independent manner.

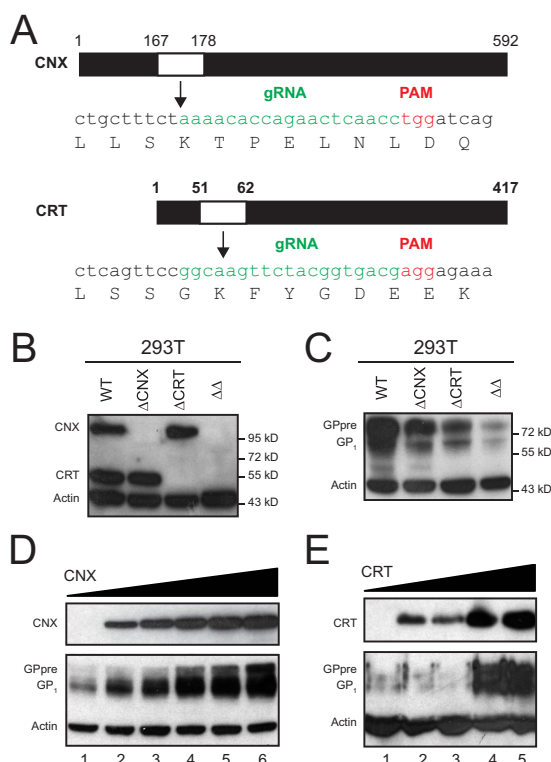


**Figure 5. Requirement of CNX/CRT for EBOV GP expression.** *A*, schematic of *CNX* and *CRT* KO by CRISPR/Cas9. The targeted gene locus of *CNX* and *CRT* is indicated by arrows. Lowercase letters present nucleotide sequences, uppercase letters represent amino acid sequences, guide RNA (gRNA) target sequences are shown in green, and the protospacer-adjacent motif (PAM) sequences are shown in red. Numbers indicate amino acid residues. *B*, detection of CNX, CRT, and actin expression by Western blotting.  $\Delta$ CNX, CNX KO cells;  $\Delta$ CRT, CRT KO cells;  $\Delta\Delta$ , CNX/CRT double KO cells. *C*, comparison of  $\Delta$ MLD-GP expression in the indicated cells by Western blotting. *D* and *E*, rescue of GP expression in CNX/CRT double KO cells by ectopic expression of CNX or CRT. Cells were transfected with  $\Delta$ MLD-GP and increasing amounts of CNX (*D*) or CRT (*E*) expression vectors, and protein expression was determined by Western blotting.

Third, we determined how GPs interact with CNX/CRT.  $\Delta$ MLD-GP and its NGS-null mutant N40Q–N618Q was expressed in WT,  $\Delta$ CNX, or  $\Delta$ CRT cells, and protein complexes were pulled down using anti-CNX or anti-CRT antibodies. It was found that both CNX and CRT could specifically pull down  $\Delta$ MLD-GP and N40Q–N618Q in WT but not  $\Delta$ CNX or  $\Delta$ CRT cells (Fig. 6, *C* and *D*). In addition, more N40Q–N618Q proteins were pulled down than WT proteins despite N40Q–N618Q protein expression being lower than the WT protein. These results demonstrate that both CNX and CRT specifically interact with EBOV GP in a *N*-glycan-independent manner.

#### Role of Asn<sup>563</sup>/Asn<sup>618</sup> in FL-GP processing and incorporation

We have shown that N563Q/N618Q mutations synergistically reduce  $\Delta$ MLD-GP processing and incorporation into HIV-1 virions. We then used FL-GP and EBOV-like particles (E-VLPs) to confirm these observations.

FL-GP and its mutants N40Q–N618Q, N40Q–N238Q, N563Q, N618Q, or N563Q/N618Q were expressed with the EBOV matrix protein VP40 in 293T WT cells, and E-VLPs were purified from the culture supernatants by ultracentrifugation. After that, viral protein expression in cells and E-VLPs was determined by Western blotting. As shown previously in Fig. 2,

the glycan-null N40Q–N618Q mutant was poorly expressed or incorporated, N40Q–N238Q mutant expression, processing, and incorporation were not affected, and the N563Q and N618Q mutations synergistically reduced FL-GP processing and incorporation into E-VLPs (Fig. 7, lanes 1–6). These results further confirm the important role of Asn<sup>563</sup> and Asn<sup>618</sup> in GP processing and incorporation.

We also performed similar experiments in CNX and/or CRT KO cells after expressing VP40 and  $\Delta$ MLD-GP bearing N40Q–N618Q, N40Q–N238Q, N563Q, N618Q, or N563Q/N618Q mutations. In general, much lower levels of GP expression were detected from these KO cells, particularly in double KO cells, which confirms the requirement of CNX/CRT for GP expression (Fig. 7, lanes 7–30). In addition, GP processing and incorporation were more strongly inhibited by these mutations in these KO cells, particularly in the double KO cells. Together, these results further demonstrate the important role of Asn<sup>563</sup>/Asn<sup>618</sup> in GP processing and incorporation.

#### The role of Asn<sup>563</sup>/Asn<sup>618</sup> in GP-mediated HIV-1 transduction

To understand how these mutations affect GP function, we determined the transduction efficiency of HIV-1-EBOV GP particles produced from 293T WT,  $\Delta$ CNX,  $\Delta$ CRT, or  $\Delta\Delta$  cells. Viruses were pseudotyped with FL-GP or  $\Delta$ MLD-GP bearing N40Q–N618Q, N40Q–N238Q, N563Q, N618Q, or N563Q/N618Q mutations. First, we analyzed how CNX/CRT affects GP function. It was found that the transduction efficiency by  $\Delta$ MLD GP was synergistically reduced by CNX and CRT KO (Fig. 8A). This result confirms the important role of CNX/CRT in EBOV GP biosynthesis. Second, we analyzed how these glycans affect GP function in WT cells. It was found that the N40Q–N238Q and N563Q mutations increased, the N618Q mutation decreased, and the N40Q–N618Q and N563Q/N618Q mutations almost completely disrupted the FL-GP and  $\Delta$ MLD-GP activities (Fig. 8, *B* and *C*). Last, we analyzed how these glycans affect GP function in CNX and/CRT KO cells. Similar results were found in these KO cells as in WT cells. For example, the N40Q–N238Q and N563Q mutants showed a comparable activity to the WT protein, which was higher than the N618Q mutant, and both the N40Q–N618Q and N563Q/N618Q mutants almost completely lost their activities (Fig. 8C). In addition, the difference between the active and inactive mutant activities was much smaller in double KO than in single KO cells (Fig. 8C). Together, these results support that Asn<sup>563</sup> and Asn<sup>618</sup> synergistically regulate EBOV GP maturation, which determines its function.

#### Discussion

In this report, we have collected new insight into how Asn<sup>563</sup> and Asn<sup>618</sup> contribute to the functionality of EBOV GP. GP<sub>1</sub> is divided into MLD, RBD, and glycan cap domain (Fig. 1A). Its crystal structure shows that the heavily glycosylated glycan cap and MLD surround the RBD, and a thick layer of oligosaccharide cloaks most of the structure (24). It was suggested that *N*-linked glycans attached to GP<sub>1</sub> might not be absolutely required for GP folding and that their function could be complemented by the other glycans in the MLD (16). When we deleted these *N*-linked glycans in  $\Delta$ MLD-GP (N40Q–N296Q),



## Functional characterization of EBOV GP N-glycosylation

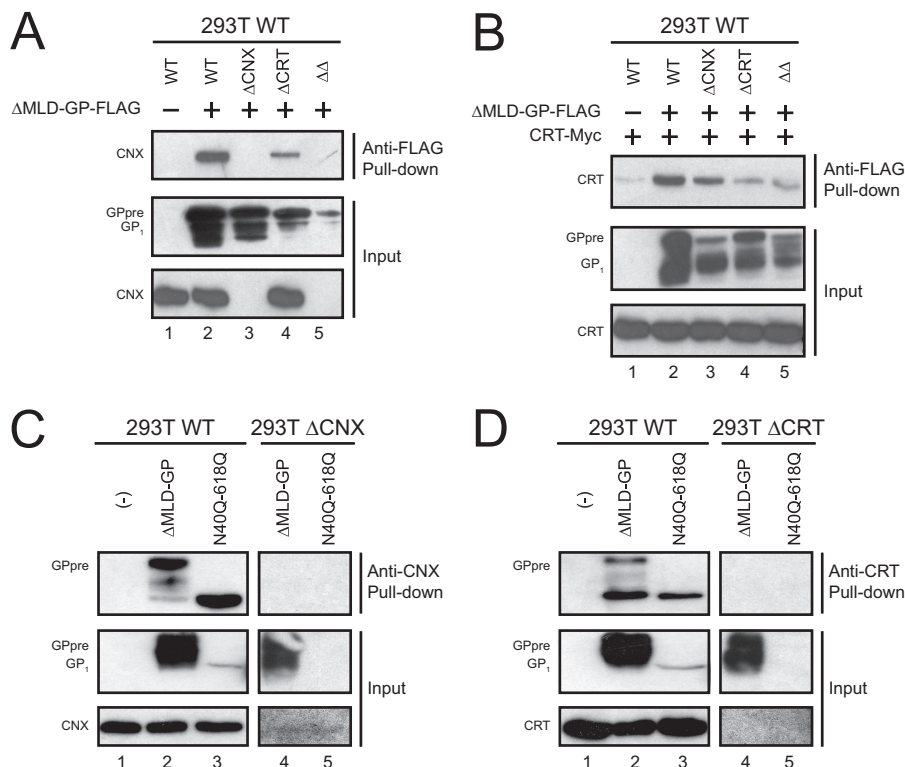


**Figure 6. Interaction of EBOV GP with CNX/CRT.** A and B, detection of GP interaction with CNX (A) or CRT (B). The indicated cells were transfected with  $\Delta$ MLD-GP expression vector alone (A) or in the presence of CRT expression vector (B). Proteins were pulled down with anti-FLAG beads and analyzed by Western blotting. C and D, role of NGGs in GP interaction with CNX and CRT. The indicated cells were transfected with WT  $\Delta$ MLD-GP or its N40Q-618Q mutant expression vector. Proteins were pulled down with anti-CN (C) or anti-CRT (D) antibodies and analyzed by Western blotting.

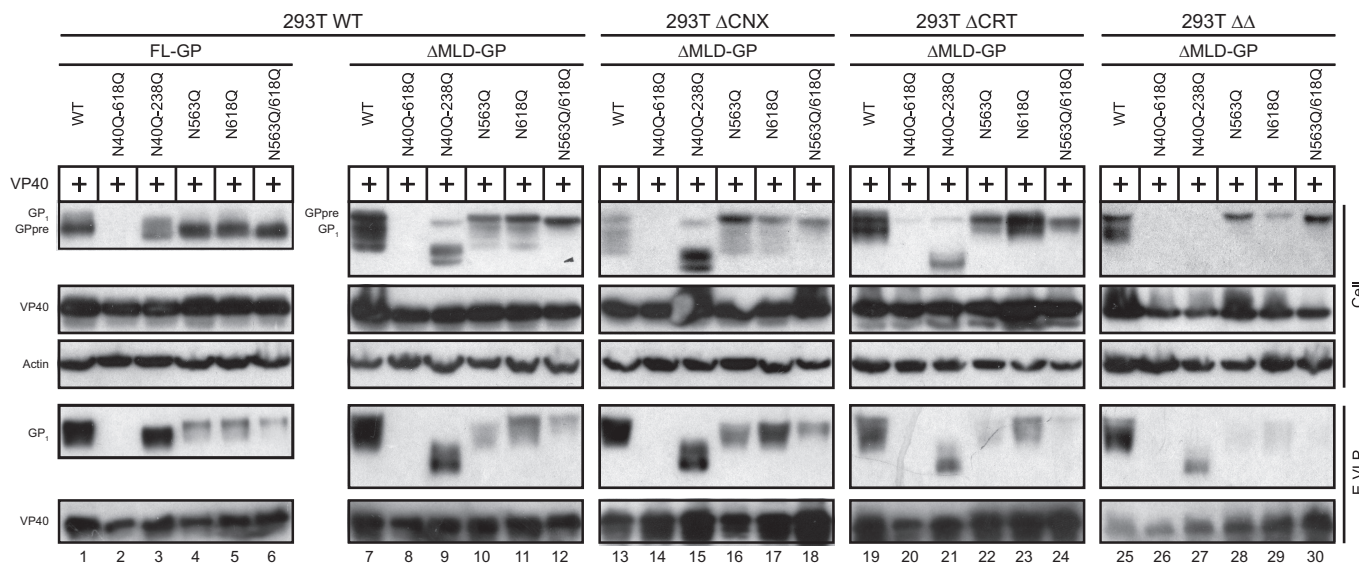


**Figure 7. Comparison of EBOV GP expression and incorporation into E-VLPs.** 293T WT,  $\Delta$ CNX,  $\Delta$ CRT, and  $\Delta\Delta$  cells were transfected with the indicated FL-GP or  $\Delta$ MLD-GP expression vectors and an EBOV matrix VP40 expression vector. E-VLPs were recovered from cell culture supernatants and purified by ultracentrifugation. Protein expression in cells and E-VLPs was analyzed by Western blotting.

we found that not only were the total levels of GP expression reduced, but GP processing and virion incorporation were also inhibited (Fig. 2, A, lane 18, and B, lane 18). Thus, our results demonstrate that these N-linked glycans become indispensable for EBOV GP expression and function when MLD is not present, confirming that the glycan cap and MLD play a complementary role in GP folding.

Unlike GP<sub>1</sub>, and independent of the MLD, N-linked glycans in GP<sub>2</sub> are required for EBOV GP function. Recent reports investigating the removal of NGGs from the FL-GP backbone show that, although an N563D mutation can enhance viral entry by 2-fold and an N618D mutation can decrease viral entry by 2-fold, an N563D/N618D double mutation is able to completely disrupt viral entry (17). Consistently, we also found that

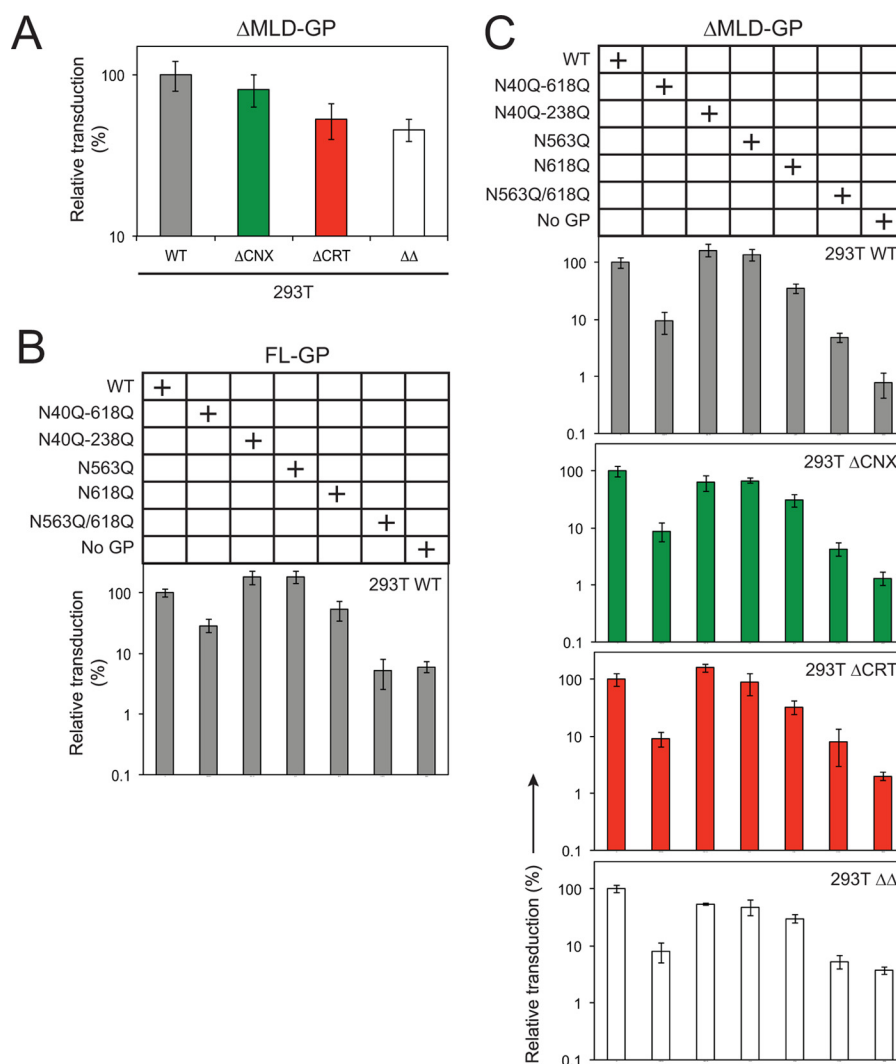


**Figure 8. Effect of NGS mutations on EBOV GP-mediated HIV-1 transduction.** A–C, HIV-1 pseudovirions were produced from 293T WT,  $\Delta$ CNX,  $\Delta$ CRT, and  $\Delta\Delta$  cells after transfection with pNL-Luc $\Delta$ Env and the  $\Delta$ MLD-GP expression vector (A), from WT cells after transfection with the HIV-1 vector and the indicated FL-GP expression vectors (B), and from WT,  $\Delta$ CNX,  $\Delta$ CRT, and  $\Delta\Delta$  cells after transfection with the HIV-1 vector and the indicated  $\Delta$ MLD-GP expression vectors (C). HIV-1 pseudovirions were collected from cell culture supernatants and normalized by the HIV-1 p24 antigen. The transduction efficiency was then determined by infecting Vero cells. Results are presented in relative values. Error bars represent standard deviation calculated from three experiments.

viral entry was slightly increased by an N563Q mutation, slightly decreased by an N618Q mutation, and almost completely disrupted by an N563Q/N618Q mutation (Fig. 8). Thus, there is conclusive evidence that glycans at Asn<sup>563</sup> impede but glycans at Asn<sup>618</sup> enhance viral entry, but simultaneous deglycosylation of both residues completely disrupts viral entry.

Although EBOV GP has a thick coating of oligosaccharides, there are vulnerable regions that are exposed to neutralizing antibodies. For example, the neutralizing antibodies KZ52 and 16F6 bind to both GP<sub>1</sub> and GP<sub>2</sub> in their prefusion complex, which may prevent their conformational rearrangements (23, 24). Their GP<sub>1</sub> epitope has been mapped to residues 42–44, and their GP<sub>2</sub> epitopes are in the internal fusion loop and HR1. Asn<sup>563</sup> and Asn<sup>618</sup> are located in HR1 or HR2, respectively. As reported before (17), we found that Asn<sup>563</sup> and/or Asn<sup>618</sup> deglycosylation reduced GP binding to KZ52 and another neutralizing antibody, 13C6 (Fig. 4, A and B). Thus, glycans at Asn<sup>563</sup> and Asn<sup>618</sup> should play an important role in GP conformational changes from prefusion to postfusion state.

To understand more about Asn<sup>563</sup> and Asn<sup>618</sup>, we performed several biochemical experiments. First, we found that both the N563Q and N618Q single mutations reduced, but the N563Q/N618Q double mutation completely blocked, GP protease cleavage (Figs. 2A and 7). Second, we found that the N563Q, N618Q, and N563Q/N618Q mutations all reduced GP incorporation (Figs. 2B and 7). Third, we found that the N563Q mutation strongly inhibited, but the N618Q mutation strongly promoted, GP trimerization; the N563Q/N618Q mutation caused a mixed phenotype by reducing trimers and increasing monomers (Fig. 4C). Nevertheless, they are not required for interaction with the ER chaperones CNX/CRT (Fig. 6). Together, these results further demonstrate that Asn<sup>563</sup>/Asn<sup>618</sup> are indeed important for the maintenance of crucial GP conformations for infection.

We also found that the N563Q, N618Q, and N563Q/N618Q mutants became highly sensitive to Endo H, indicating that they should contain high-Man sugars (Fig. 3A). Demannosylation is an essential step during N-glycosylation, which remodels the

## Functional characterization of EBOV GP N-glycosylation

sugar chains by removing Man residues and adding other sugars. *N*-glycosylation produces three types of structures: high-Man, hybrid, and complex (25). The high-Man and some hybrid types contain more Man residues than the complex type, which are cleavable by Endo H. Previously, it has been taken as common knowledge that glycoproteins with high-Man structures could not be released from the ER, so Endo H resistance was used as a marker for trafficking to the Golgi (26). However, recent findings have uncovered that many glycoproteins with high-Man sugars are indeed secreted to the cell surface, suggesting that these proteins can exit from the ER (27). Interestingly, it was reported before that loss of two NGGs on rabies virus GPs also resulted in production of high-Man glycoprotein without affecting cell surface expression (28, 29). In addition, it was reported that high-Man glycans on Env reduce HIV-1 infectivity and block mucosal transmission of simian immunodeficiency virus (SIV) (30–32). Moreover, SIV Env incorporation is profoundly impaired when Env is modified by high-Man structure glycans (32). To understand whether the high-Man structure also reduces EBOV GP-mediated transduction, we treated viral producer cells with KIF to block demannosylation. We found that the treatment indeed not only blocked demannosylation (Fig. 3B) but also reduced transduction in a dose-dependent manner (Fig. 3C). Thus, because the high-Man oligosaccharides represent an incompletely processed, immature *N*-glycan structure, they may negatively modulate EBOV GP function via a similar mechanism as that in HIV-1 and SIV.

We observed a striking inconsistency between levels of GP incorporation and transduction efficiency. For example, although both the N563Q and N563Q/N618Q mutants were poorly incorporated (Fig. 2B, lanes 9 and 25), only the N563Q/N618Q mutant significantly lost transduction efficiency, and the N563Q mutant showed a slight increase in efficiency relative to the WT protein (Fig. 8). As introduced earlier, EBOV infection requires very low levels of GP on the virus surface, and high levels of GP strongly reduce viral titers (14). Thus, our results confirm that a very low level of incorporated GP is sufficient for EBOV infection. In addition, our results also suggest that levels of EBOV GP incorporation should not be viewed as a reflective criterion for its transduction efficiency.

In summary, we have observed dramatic changes in EBOV GP biochemical properties via deglycosylation of Asn<sup>563</sup>/Asn<sup>618</sup>, which include processing, demannosylation, and oligomerization. These changes synergistically affect EBOV GP conformation and disrupt viral entry. Thus, Asn<sup>563</sup>/Asn<sup>618</sup> represent an attractive target to block EBOV infection.

### Experimental procedures

#### Enzyme, inhibitor, and antibodies

Endo H was purchased from New England Biolabs. KIF, radioimmune precipitation assay (RIPA) lysis buffer, anti-FLAG M2 antibodies, anti-FLAG affinity gel, and anti-HA antibodies were purchased from Sigma-Aldrich. Anti-actin and anti-C-Myc monoclonal antibodies were purchased from Santa Cruz Biotechnology. Rabbit anti-calnexin polyclonal antibodies were purchased from Enzo Life Science. Anti-calreticulin monoclonal antibodies were purchased from Cell Signaling

Technology. Anti-Zaire EBOV VP40 rabbit polyclonal antibody was purchased from Sino Biological. Allophycocyanin-conjugated mouse anti-FLAG antibody was purchased from Columbia Biosciences. KZ52 and 13C6 antibodies were purchased from IBT Bioservices. Phycoerythrin-conjugated goat anti-human IgG secondary antibody was purchased from Santa Cruz Biotechnology. HRP-conjugated secondary antibodies for Western blotting were purchased from Jackson ImmunoResearch Laboratories. The anti-HIV-1 Gag monoclonal antibody (183) was obtained from the National Institutes of Health AIDS Research and Reference Reagent Program.

#### Plasmids

The HIV-Luc reporter proviral vector pNL-Luc-ΔEnv was described before (33). The N-terminal FLAG-tagged EBOV ΔMLD GP expression vector was obtained from Shan-Lu Liu (University of Missouri). The human codon-optimized Cas9 expression vector was obtained from George M. Church (Harvard Medical School) through Addgene. pEGFP-C1 was purchased from Clontech. A plasmid expressing the full-length EBOV Zaire subtype matrix VP40 was purchased from Sino Biological.

To create calnexin- and calreticulin-expressing constructs, the nucleotide sequences encoding HA-tagged calnexin and C-Myc-tagged calreticulin were amplified by PCR from pMSCVneo-CANX (34) and pCMV6-CRT (Origene), respectively, and subcloned into the pCAGGS vector. To generate the FL-GP expression vector, the coding sequence for GP MLD was first synthesized and then inserted into the ΔMLD-GP expression vector via overlapping PCR. Single *N*-glycosylation mutants were constructed by asparagine-to-glutamine substitution using the QuikChange site-directed mutagenesis kit (Agilent Technologies). Single *N*-glycosylation mutants were subjected to further rounds of mutagenesis to create multiple sites mutants. All vectors were sequenced to confirm the correct sequences. Detailed procedures for the construction of the plasmids are available upon request.

#### Cells

The 293T, HeLa, and Vero cell lines were purchased from the ATCC and maintained in DMEM supplemented with 10% fetal bovine serum, 100 units/ml penicillin, and 100 μg/ml streptomycin (Gibco) at 37 °C in 5% CO<sub>2</sub>.

#### Virus production

Lentiviral pseudovirions bearing EBOV GP were generated as described before with minor modifications (35). Briefly, a total of 4 × 10<sup>6</sup> 293T cells were seeded in 10-cm dishes and cultured overnight. Five micrograms of the plasmid encoding either the WT or mutant EBOV GP and 5 μg of pNL-Luc-ΔEnv were mixed with 30 μl of PEI (Polysciences, 1 μg/μl) in 500 μl of serum-free DMEM. After a 15-min incubation at room temperature, the transfection complexes were added to the cells. The medium was replaced with fresh medium 6 h after transfection. Forty-eight hours later, the culture supernatants were collected, clarified by low-speed centrifugation, and passed through a 0.45-μm syringe filter to remove any cell debris. The virion-containing supernatants were either used to infect target

cells or stored at  $-80^{\circ}\text{C}$ . E-VLPs were generated by the same method, except that the pNL-Luc- $\Delta\text{Env}$  vector was replaced with a VP40-encoding plasmid. To analyze the levels of EBOV GP incorporation, supernatants containing virions were centrifuged at 25,000 rpm at  $4^{\circ}\text{C}$  for 2 h using a Beckman SW-32Ti rotor. Viral pellets were resuspended in RIPA buffer and subjected to Western blotting analysis.

#### EBOV transduction assay

A total of  $2 \times 10^4$  Vero cells were seeded in each well of 96-well plates 24 h prior to infection. An equal amount of pseudoviruses (normalized by HIV p24<sup>Gag</sup>) was inoculated into these cells. After 48 h of infection, the culture medium was removed, and cells were lysed in 100  $\mu\text{l}$  of lysis buffer (Promega). Luminescence was measured with a luciferase assay kit (Promega) and a TD-20/20 luminometer (Turner Designs).

#### Western blotting and immunoprecipitation

After being washed three times with cold PBS, transfected cells were lysed in RIPA buffer supplemented with 1 mg/ml protease inhibitor mixture (Roche) for 30 min on ice. Lysate was centrifuged at  $12,000 \times g$  for 10 min at  $4^{\circ}\text{C}$  to remove any debris. Clarified supernatants were mixed with DTT-containing sample loading buffer (Solarbio), heated at  $95^{\circ}\text{C}$  for 5 min, and then resolved by PAGE in 10% gels under reducing conditions. Some samples were subjected to Endo H treatment before applying them to the SDS-PAGE. To do so, a total of 20  $\mu\text{g}$  of lysate was first denatured by heating at  $100^{\circ}\text{C}$  for 10 min in denaturing buffer. Denatured proteins were added to a 20- $\mu\text{l}$  reaction system containing 2  $\mu\text{l}$  of GlycoBuffer and 1000 units of Endo H and incubated at  $37^{\circ}\text{C}$  for 1 h.

For blue native PAGE, samples were prepared in native PAGE buffer (Life Technology) and separated on Novex 3–12% BisTris gels (Invitrogen) according to the protocol of the manufacturer.

For immunoprecipitation, clarified cell lysate was incubated with antibodies followed by addition of protein G-Sepharose beads (Pierce) or directly with anti-FLAG M2 monoclonal antibody-coupled beads (Sigma) at  $4^{\circ}\text{C}$  for 4 h with rotation. Beads were washed twice with cold PBS containing 1% Triton X-100, followed by one more washing with PBS alone. Proteins were then eluted from beads by boiling and separated under denaturing conditions.

For Western blotting, gels from reducing or non-reducing electrophoresis were transferred to PVDF membranes. Membranes were briefly blocked with TBS containing 5% skim milk and 0.1% Tween 20 and then incubated with primary antibodies for 1 h at room temperature by the following dilutions: anti-FLAG antibody, 1:2000; anti-HA antibody, 1:3000; anti-Myc antibody, 1:1000; anti-CNX antibody, 1:1000; anti-CRT antibody, 1:1000; and anti-HIV p24 antibody, 1:3000. After being washed further with TBS containing 0.1% Tween 20, membranes were incubated with HRP-conjugated secondary antibodies at a 1:10,000 dilution. Chemiluminescence was detected by incubating the membrane with SuperSignal substrate (Pierce).

#### Gene knockout

The CRISPR/Cas9 system was employed to knock out *CNX* and/or *CRT* genes in 293T cells as described before (36, 37). Briefly, a DNA fragment that contained the U6 promoter, a 19-bp target sequence specific for *CNX* or *CRT*, a guide RNA scaffold, and a U6 termination signal sequence was synthesized and subcloned into the pGEM-T Easy vector (Promega). The vector was transfected with the human codon-optimized Cas9 expression vector and pEGFP-C1 into 293T cells. Twenty-four hours later, GFP-positive cells were isolated by fluorescence-activated cell sorting and subjected to cloning by limiting dilution. After 10–14 days, knockout clones were identified after screening by Western blotting.

#### Flow cytometry

For cell surface GP staining, a total of  $1 \times 10^6$  293T cells were transfected with EBOV GP expression vector. Forty-eight hours later, cells were harvested and washed twice with PBS containing 0.1% bovine serum albumin. Cells were stained with allophycocyanin-conjugated anti-FLAG antibody for 30 min at  $4^{\circ}\text{C}$ , washed three times, fixed in 4% paraformaldehyde, and analyzed by FACScan (BD Biosciences). Cells were also incubated with KZ52 or 13C6, followed by staining with phycoerythrin-conjugated anti-human IgG antibodies. The negative gate was defined with untransfected cells stained with the same antibody.

**Author contributions**—B. W. and Y. H. Z. designed the study and wrote the paper. Y. W., B. W., D. A. F., X. Z., X. Y., D. H., Z. Z., C. L., and S. Z. performed the experiments. S. H. X. provided comments regarding the paper. All authors analyzed the results and approved the final version of the manuscript.

**Acknowledgments**—We thank Shan-Lu Liu, George M. Church, and the National Institutes of Health AIDS Research and Reference Reagent Program for providing various reagents. We also thank Xianfeng Zhang, Honglin Jia, Li Jiang, and Yue Wang for helpful discussions and Xinghe Wang, Qun Yu, and Nana Yi for technical assistance.

#### References

1. Vygen, S., Tiffany, A., Rull, M., Ventura, A., Wolz, A., Jambai, A., and Porten, K. (2016) Changes in health-seeking behavior did not result in increased all-cause mortality during the Ebola outbreak in Western Area, Sierra Leone. *Am. J. Trop. Med. Hyg.* **95**, 897–901
2. Feldmann, H., and Geisbert, T. W. (2011) Ebola haemorrhagic fever. *Lancet* **377**, 849–862
3. Cook, J. D., and Lee, J. E. (2013) The secret life of viral entry glycoproteins: moonlighting in immune evasion. *PLoS Pathog.* **9**, e1003258
4. Takada, A., Robison, C., Goto, H., Sanchez, A., Murti, K. G., Whitt, M. A., and Kawaoka, Y. (1997) A system for functional analysis of Ebola virus glycoprotein. *Proc. Natl. Acad. Sci. U.S.A.* **94**, 14764–14769
5. Wool-Lewis, R. J., and Bates, P. (1998) Characterization of Ebola virus entry by using pseudotyped viruses: identification of receptor-deficient cell lines. *J. Virol.* **72**, 3155–3160
6. Podbilewicz, B. (2014) Virus and cell fusion mechanisms. *Annu. Rev. Cell Dev. Biol.* **30**, 111–139
7. Yang, Z. Y., Duckers, H. J., Sullivan, N. J., Sanchez, A., Nabel, E. G., and Nabel, G. J. (2000) Identification of the Ebola virus glycoprotein as the main viral determinant of vascular cell cytotoxicity and injury. *Nat. Med.* **6**, 886–889

## Functional characterization of EBOV GP N-glycosylation

- Sanchez, A., Trappier, S. G., Mahy, B. W., Peters, C. J., and Nichol, S. T. (1996) The virion glycoproteins of Ebola viruses are encoded in two reading frames and are expressed through transcriptional editing. *Proc. Natl. Acad. Sci. U.S.A.* **93**, 3602–3607
- Volchkov, V. E., Becker, S., Volchkova, V. A., Ternovoj, V. A., Kotov, A. N., Netesov, S. V., and Klenk, H. D. (1995) GP mRNA of Ebola virus is edited by the Ebola virus polymerase and by T7 and vaccinia virus polymerases. *Virology* **214**, 421–430
- Mohan, G. S., Li, W., Ye, L., Compans, R. W., and Yang, C. (2012) Antigenic subversion: a novel mechanism of host immune evasion by Ebola virus. *PLoS Pathog.* **8**, e1003065
- Volchkov, V. E., Feldmann, H., Volchkova, V. A., and Klenk, H. D. (1998) Processing of the Ebola virus glycoprotein by the proprotein convertase furin. *Proc. Natl. Acad. Sci. U.S.A.* **95**, 5762–5767
- Dolnik, O., Volchkova, V., Garten, W., Carbonnelle, C., Becker, S., Kahnt, J., Ströher, U., Klenk, H. D., and Volchkov, V. (2004) Ectodomain shedding of the glycoprotein GP of Ebola virus. *EMBO J.* **23**, 2175–2184
- Jeffers, S. A., Sanders, D. A., and Sanchez, A. (2002) Covalent modifications of the Ebola virus glycoprotein. *J. Virol.* **76**, 12463–12472
- Mohan, G. S., Ye, L., Li, W., Monteiro, A., Lin, X., Sapkota, B., Pollack, B. P., Compans, R. W., and Yang, C. (2015) Less is more: Ebola virus surface glycoprotein expression levels regulate virus production and infectivity. *J. Virol.* **89**, 1205–1217
- Sanchez, A., Yang, Z. Y., Xu, L., Nabel, G. J., Crews, T., and Peters, C. J. (1998) Biochemical analysis of the secreted and virion glycoproteins of Ebola virus. *J. Virol.* **72**, 6442–6447
- Lennemann, N. J., Rhein, B. A., Ndungo, E., Chandran, K., Qiu, X., and Maury, W. (2014) Comprehensive functional analysis of N-linked glycans on Ebola virus GP1. *MBio* **5**, e00862–00813
- Lennemann, N. J., Walkner, M., Berkebile, A. R., Patel, N., and Maury, W. (2015) The role of conserved N-linked glycans on Ebola virus glycoprotein 2. *J. Infect. Dis.* **212**, S204–209
- Helenius, A., and Aebi, M. (2004) Roles of N-linked glycans in the endoplasmic reticulum. *Annu. Rev. Biochem.* **73**, 1019–1049
- Williams, D. B. (2006) Beyond lectins: the calnexin/calreticulin chaperone system of the endoplasmic reticulum. *J. Cell Sci.* **119**, 615–623
- Wu, Y., Swilius, M. T., Moremen, K. W., and Sifers, R. N. (2003) Elucidation of the molecular logic by which misfolded  $\alpha$  1-antitrypsin is preferentially selected for degradation. *Proc. Natl. Acad. Sci. U.S.A.* **100**, 8229–8234
- Maruyama, T., Rodriguez, L. L., Jahrling, P. B., Sanchez, A., Khan, A. S., Nichol, S. T., Peters, C. J., Parren, P. W., and Burton, D. R. (1999) Ebola virus can be effectively neutralized by antibody produced in natural human infection. *J. Virol.* **73**, 6024–6030
- Wilson, J. A., Hevey, M., Bakken, R., Guest, S., Bray, M., Schmaljohn, A. L., and Hart, M. K. (2000) Epitopes involved in antibody-mediated protection from Ebola virus. *Science* **287**, 1664–1666
- Dias, J. M., Kuehne, A. I., Abelson, D. M., Bale, S., Wong, A. C., Halfmann, P., Muhammad, M. A., Fusco, M. L., Zak, S. E., Kang, E., Kawaoka, Y., Chandran, K., Dye, J. M., and Saphire, E. O. (2011) A shared structural solution for neutralizing ebolaviruses. *Nat. Struct. Mol. Biol.* **18**, 1424–1427
- Lee, J. E., Fusco, M. L., Hessel, A. J., Oswald, W. B., Burton, D. R., and Saphire, E. O. (2008) Structure of the Ebola virus glycoprotein bound to an antibody from a human survivor. *Nature* **454**, 177–182
- Kornfeld, R., and Kornfeld, S. (1985) Assembly of asparagine-linked oligosaccharides. *Annu. Rev. Biochem.* **54**, 631–664
- Willey, R. L., Maldarelli, F., Martin, M. A., and Strebel, K. (1992) Human immunodeficiency virus type 1 Vpu protein induces rapid degradation of CD4. *J. Virol.* **66**, 7193–7200
- MacLeod, D. T., Choi, N. M., Briney, B., Garces, F., Ver, L. S., Landais, E., Murrell, B., Wrin, T., Kilembe, W., Liang, C. H., Ramos, A., Bian, C. B., Wickramasinghe, L., Kong, L., Eren, K., et al. (2016) Early antibody lineage diversification and independent limb maturation lead to broad HIV-1 neutralization targeting the Env high-mannose patch. *Immunity* **44**, 1215–1226
- Wojczyk, B. S., Takahashi, N., Levy, M. T., Andrews, D. W., Abrams, W. R., Wunner, W. H., and Spitalnik, S. L. (2005) N-glycosylation at one rabies virus glycoprotein sequon influences N-glycan processing at a distant sequon on the same molecule. *Glycobiology* **15**, 655–666
- Wojczyk, B. S., Stwora-Wojczyk, M., Shakin-Eshleman, S., Wunner, W. H., and Spitalnik, S. L. (1998) The role of site-specific N-glycosylation in secretion of soluble forms of rabies virus glycoprotein. *Glycobiology* **8**, 121–130
- Gaskill, P. J., Zandonatti, M., Gilmartin, T., Head, S. R., and Fox, H. S. (2008) Macrophage-derived simian immunodeficiency virus exhibits enhanced infectivity by comparison with T-cell-derived virus. *J. Virol.* **82**, 1615–1621
- Shen, R., Raska, M., Bimczok, D., Novak, J., and Smith, P. D. (2014) HIV-1 envelope glycan moieties modulate HIV-1 transmission. *J. Virol.* **88**, 14258–14267
- Karsten, C. B., Buettner, F. F., Cajic, S., Nehlmeier, I., Neumann, B., Klippert, A., Sauermann, U., Reichl, U., Gerardy-Schahn, R., Rapp, E., Stahl-Hennig, C., and Pöhlmann, S. (2015) Exclusive decoration of simian immunodeficiency virus Env with high-mannose type N-glycans is not compatible with mucosal transmission in rhesus macaques. *J. Virol.* **89**, 11727–11733
- Zhou, T., Dang, Y., Baker, J. J., Zhou, J., and Zheng, Y. H. (2012) Evidence for Vpr-dependent HIV-1 replication in human CD4+ CEM.NKR T-cells. *Retrovirology* **9**, 93
- Zhou, T., Han, Y., Dang, Y., Wang, X., and Zheng, Y. H. (2009) A novel HIV-1 restriction factor that is biologically distinct from APOBEC3 cytidine deaminases in a human T cell line CEM.NKR. *Retrovirology* **6**, 31
- Manicassamy, B., Wang, J., Jiang, H., and Rong, L. (2005) Comprehensive analysis of Ebola virus GP1 in viral entry. *J. Virol.* **79**, 4793–4805
- Zhou, T., Dang, Y., and Zheng, Y. H. (2014) The mitochondrial translocator protein, TSPO, inhibits HIV-1 envelope glycoprotein biosynthesis via the endoplasmic reticulum-associated protein degradation pathway. *J. Virol.* **88**, 3474–3484
- Zhou, T., Frabutt, D. A., Moremen, K. W., and Zheng, Y. H. (2015) ER-ManI (endoplasmic reticulum class I  $\alpha$ -mannosidase) is required for HIV-1 envelope glycoprotein degradation via endoplasmic reticulum-associated protein degradation pathway. *J. Biol. Chem.* **290**, 22184–22192

**Mechanistic understanding of *N*-glycosylation in Ebola virus glycoprotein maturation and function**

Bin Wang, Yujie Wang, Dylan A. Frabutt, Xihe Zhang, Xiaoyu Yao, Dan Hu, Zhuo Zhang, Chaonan Liu, Shimin Zheng, Shi-Hua Xiang and Yong-Hui Zheng

*J. Biol. Chem.* 2017, 292:5860-5870.

doi: 10.1074/jbc.M116.768168 originally published online February 14, 2017

---

Access the most updated version of this article at doi: [10.1074/jbc.M116.768168](https://doi.org/10.1074/jbc.M116.768168)

Alerts:

- [When this article is cited](#)
- [When a correction for this article is posted](#)

[Click here](#) to choose from all of JBC's e-mail alerts

Supplemental material:

<http://www.jbc.org/content/suppl/2017/02/14/M116.768168.DC1>

This article cites 37 references, 20 of which can be accessed free at <http://www.jbc.org/content/292/14/5860.full.html#ref-list-1>